Title	Damage detection using curvatures obtained from vehicle measurements
Authors(s)	O'Brien, Eugene J., Martinez, Daniel, Malekjafarian, Abdollah, Sevillano, Enrique
Publication date	2017-07
Publication information	O’Brien, Eugene J., Daniel Martinez, Abdollah Malekjafarian, and Enrique Sevillano. “Damage Detection Using Curvatures Obtained from Vehicle Measurements.” Springer, July 2017. https://doi.org/10.1007/s13349-017-0233-8.
Publisher	Springer
Item record/more information	http://hdl.handle.net/10197/8754
Publisher's statement	The final publication is available at Springer via http://dx.doi.org/10.1007/s13349-017-0233-8
Publisher's version (DOI)	10.1007/s13349-017-0233-8

Damage Detection Using Curvatures obtained from Vehicle Measurements

Eugene J. OBrien[1], Daniel Martinez[1], Abdollah Malekjafarian [1], Enrique Sevillano[1]

[1] *School of Civil Engineering, University College Dublin, Dublin 4, Ireland*

Abstract

This paper describes a new procedure for bridge damage identification through drive-by monitoring. Instantaneous Curvature (IC) is presented as a means to determine a local loss of stiffness in a bridge through measurements collected from a passing instrumented vehicle. Moving Reference Curvature (MRC) is compared with IC as a damage detection tool. It is assumed that absolute displacements on the bridge can be measured by the vehicle. The bridge is represented by a finite element (FE) model. A Half-car model is used to represent the passing vehicle. Damage is represented as a local loss of stiffness in different parts of the bridge. 1% random noise and no noise environments are considered to evaluate the effectiveness of the method. A generic road surface profile is also assumed. Numerical simulations show that the local damage can be detected using IC if the deflection responses can be measured with sufficient accuracy. Damage quantification can be obtained from MRC.

Keywords: Bridge; Drive-by; Damage Detection; Structural Health Monitoring; SHM; Instantaneous Curvature; Moving Reference Curvature.

Corresponding author's email: daniel.martinezotero@ucd.ie

Introduction

There is an increasing demand for improved monitoring of the condition of structures, which is commonly referred to as Structural Health Monitoring (SHM) [1-4]. Advances in computation in the last 20 years along with deterioration and ageing of structures have contributed to significant development of SHM. An effective SHM plan operates at some or all of the following levels [5]: (i) occurrence, (ii) location, (iii) and severity of damage and (iv) prediction of remaining service life. Many researchers have applied SHM methods for civil engineering structures [6-9]. Several methods have been developed for SHM of bridges as critical components of transport infrastructure [10-13].

Visual inspection and sensor based monitoring are common practice in bridge management. Methods based on visual inspection are expensive and may not provide reliable results so there is a trend of increasing use of bridge instrumentation. Bridge instrumentation involving a power source, data acquisition electronics and many sensors is already common practice for bridge damage detection in larger bridges [10, 14-16]. This approach is known as direct monitoring [17, 18]. It is more easily justified for long-span bridges, since its cost does not represent a high percentage of the overall capital cost. The quantity of sensors and the need for data acquisition and power on each bridge make direct bridge monitoring uneconomical for most short span bridges [19]. Yang et. al [20, 21] proposed drive-by or indirect bridge monitoring, in which the bridge condition is evaluated using the response measured on a passing vehicle [22]. It is particularly promising for short and medium span bridges. Several methods have been proposed in recent years using indirect measurements for damage detection purposes [23-27].

Five damage identification parameters can be highlighted: (i) frequency [28-30], (ii) damping [31-33], (iii) mode shapes [30, 34, 35], (iv) accelerations [36-38] and (v) curvatures. Curvature methods are usually focused on the mode shape and the deflection [39]. Zhang et al. [40] have developed a new algorithm using mode shape curvatures obtained from indirect measurements. Sun et al. [41] consider the vehicle as an exciter only, using a displacement transducer to measure the deflection at a specific position. Curvature is related to bending moment and stiffness and it can, at least theoretically, be derived from deflection measurements taken from a passing vehicle. As loss of stiffness can be expressed as damage, curvature has been identified as a promising property for damage detection [39, 42, 43].

The Traffic Speed Deflectometer (TSD) is a vehicle that can take measurements when moving at a constant speed of 72 to 80 km/h [44, 45]. The application of TSD for pavement monitoring has been investigated by Rada et al. [46]. It uses a set of Doppler laser vibrometers to measure the vertical velocity between vehicle and road profile under the rear-right tyre [47]. OBrien & Keenahan [25] first propose the use of a TSD for drive-by bridge monitoring, but do not address the issue of finding absolute deflection measurements from the measured relative velocities.

In this paper, Instantaneous Curvature (IC) and Moving Reference Curvature (MRC), first proposed in [48], are tested for two damage scenarios. It is assumed that the relative deflection between the TSD and the pavement surface of the bridge can be found from the laser vibrometer measurements. Vehicle bridge interaction is modelled using a Finite Element (FE) model. The vehicle is represented by a Half-car model, and the bridge by an Euler-Bernoulli beam. The first damage case includes a local loss of stiffness at a single point on the bridge and the second case involves damage at two points. Noise-free and 1% noise cases are evaluated. A Difference Ratio (DR) is introduced for damage localisation using IC and a least squares method is suggested for MRC. It is shown that both methods can detect the damage location with acceptable accuracy.

Vehicle-Bridge Interaction model

A Finite Element (FE) model is employed to simulate Vehicle-Bridge Interaction (VBI). In this model, VBI is represented as a coupled system which is a well-accepted approach in the literature [32, 34, 49]. A Half-car model with 4 degrees of freedom (DOFs) is implemented in MATLAB to simulate the interaction between the vehicle and the bridge. The Half-car model is demonstrated to be a suitable model representing a vehicle [50] and has been used widely in the literature [34, 51]. These DOFs are related to body bounce translation (y_s), body pitch rotation (θ_s) and the two axle vertical translations (u_{u1} and u_{u2}). m_{u1},m_{u2} and m_s typify respectively the two axle sprung masses and the vehicle body mass, representing the gross mass of the vehicle. $K_{t,1}$ and $K_{t,2}$ represent the two tyre stiffnesses. $K_{s,1}$ and $K_{s,2}$ represent the suspension stiffnesses and $C_{s,1}$,$C_{s,2}$ represent the damping of the suspensions. As the vehicle travels from left to right, the deflection responses are measured using three sensors located near the second axle. The central sensor is at a distance, x, from the start of the bridge and the other two sensors are at a distance, Δx (= 1m), on either side of it – see Fig.1. In this paper, the Half-car passes over the bridge which is modelled using 40 elements, each 0.5 m long (Fig. 1).

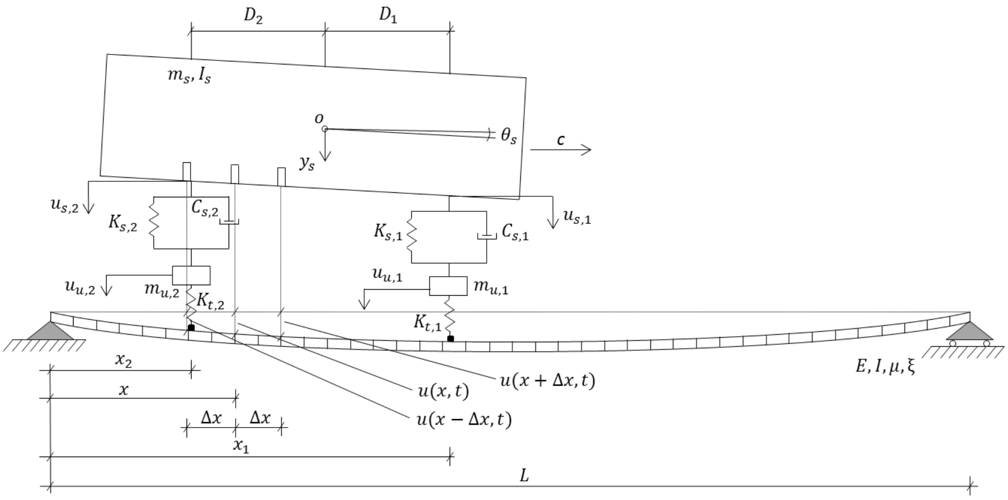

Figure 1. A Half-car model on a simply supported beam, adapted from [18].

The bridge is modelled as a simply supported beam using the FE method. Each element includes two nodes and four degrees of freedom. Both bridge and vehicle must obey the general dynamic equation of equilibrium:

$$M\ddot{u} + C\dot{u} + Ku = F \tag{1}$$

where F is the force applied to the system, M is the mass matrix, C is the damping matrix and K is the stiffness matrix. Vectors u, $\dot{u}$ and $\ddot{u}$ represent the displacement, velocity and acceleration. Different dynamic equations must be considered for the vehicle and the bridge:

$$M_v\ddot{u}_v + C_v\dot{u}_v + K_v u_v = f_{int} \tag{2}$$

$$M_b\ddot{u}_b + C_b\dot{u}_b + K_b u_b = f_{int} \tag{3}$$

where f_{int} is the interaction force vector applied to the vehicle DOFs at each instant of time, u_v is the vehicle's displacement, u_b is the bridge's displacement, M_b is the mass matrix of the bridge, C_b is the damping matrix and K_b is the stiffness matrix. The vehicle mass matrix M_v, damping matrix C_v and stiffness matrix K_v are given by:

$$M_v = \begin{bmatrix} m_s & 0 & 0 & 0 \\ 0 & I_s & 0 & 0 \\ 0 & 0 & m_{u,1} & 0 \\ 0 & 0 & 0 & m_{u,2} \end{bmatrix} \tag{4}$$

$$C_v = \begin{bmatrix} C_{s,1} + C_{s,2} & D_1C_{s,1} - D_2C_{s,2} & -C_{s,1} & -C_{s,2} \\ D_1C_{s,1} - D_2C_{s,2} & {D_1}^2C_{s,1} + {D_2}^2C_{s,2} & -D_1C_{s,1} & D_2C_{s,2} \\ -C_{s,1} & -D_1C_{s,1} & C_{s,1} & 0 \\ -C_{s,2} & D_2C_{s,2} & 0 & C_{s,2} \end{bmatrix} \tag{5}$$

$$K_v = \begin{bmatrix} K_{s,1} + K_{s,2} & D_1K_{s,1} - D_2K_{s,2} & -K_{s,1} & -K_{s,2} \\ D_1K_{s,1} - D_2K_{s,2} & {D_1}^2K_{s,1} + {D_2}^2K_{s,2} & -D_1K_{s,1} & D_2K_{s,2} \\ -K_{s,1} & -D_1K_{s,1} & K_{s,1} & 0 \\ -K_{s,2} & D_2K_{s,2} & 0 & K_{s,2} \end{bmatrix} \tag{6}$$

Consistent elemental mass matrix and stiffness matrix have been applied to create the bridge mass matrix M_b and the bridge stiffness matrix K_b [52]. The damping ratio (ξ) for civil engineering structures in general is very low. In the bridge model, damping is simulated with the Rayleigh damping assumption. Bridge damping, C_b, is estimated as a linear function of stiffness and mass with coefficients α and β:

$$C_b = \alpha M_b + \beta K_b \tag{7}$$

Clough et al. [53] state that α and β can be estimated using the following:

$$\alpha = \frac{2\xi\omega_1\omega_2}{\omega_1+\omega_2} \tag{8}$$

$$\beta = \frac{2\xi}{\omega_1+\omega_2} \tag{9}$$

where ω_1 and ω_2 are the first and second natural frequencies of the bridge.
The interaction force vector f_{int} is applied to the bridge due to the vehicle's load. For a given measuring frequency, a time step can be obtained. At every time step, the force is distributed between the DOFs, as shown in Fig. 1. Hermitian shape functions are executed for this purpose [52].

A steady contact between tyre and bridge is considered in the Half-car model, where the relation between vehicle and bridge interaction forces can be established. The global dynamic equation can be formulated using this assumption and from Eq. 1:

$$M_g\ddot{u} + C_g\dot{u} + K_g u = F \tag{10}$$

where u represents the displacement of the global system and coupled mass, damping and stiffness matrices, defined as:

$$M_g = \begin{bmatrix} M_v & 0 \\ 0 & M_b \end{bmatrix}_{(n+4)\times(n+4)} \tag{11}$$

$$C_g = \begin{bmatrix} C_v & 0 \\ 0 & C_b \end{bmatrix}_{(n+4)\times(n+4)} \tag{12}$$

$$K_g = \begin{bmatrix} K_{vv} & K_{vb} \\ K_{bv} & K_b + K_{bb} \end{bmatrix}_{(n+4)\times(n+4)} \tag{13}$$

where n represents the number of DOFs in the bridge model. The dimension of the global matrices is logically the sum of that in the vehicle and the bridge's matrices. Stiffness global matrix K_g is time dependent and its components are obtained by combining the previous equation with the influence of the tyre. The force vector couples the vehicle and the bridge:

$$F = \begin{Bmatrix} 0 \\ 0 \\ K_{t,1}r_1 \\ K_{t,2}r_2 \\ N_b \begin{Bmatrix} P_1 - K_{t,1}r_1 \\ P_2 - K_{t,2}r_2 \end{Bmatrix} \end{Bmatrix}_{(n+4)\times 1} \tag{14}$$

where N_b is the location matrix, r_1 and r_2 are the road profile displacements under each axle, P_1 and P_2 are the static axle loads of the vehicle and $K_{t,1}$ and $K_{t,2}$ are the tyre stiffnesses.

Displacements, velocities and accelerations for both bridge and vehicle are calculated using the Wilson-Theta scheme of integration defined in Tedesco's book [54]. The Wilson-Theta method is a more complex approach than linear acceleration integration. The improvement of the Wilson-Theta method consists of using a value of θ for the estimation of an unknown point. $\theta = 1$ results in a linear acceleration approach. The recommended value for θ has to be $\theta \geq 1.37$ for unconditional stability [54]. Here, a value of $\theta = 1.420815$ is used.

The properties of the vehicle and the bridge are given in Tables 1 and 2 respectively. The vehicle properties are provided by the manufacturer of the TSD. The road surface profile shown in Fig. 2 is considered. A constant velocity of 72 km/h is assumed for the Half-car to simulate highway conditions for the vehicle. A 10-m approach road before the bridge is also assumed.

Table 1. Geometrical and mechanical properties of the vehicle

Half-car property	Notation	Value
Weight of the sprung mass	m_s	9 t
Unsprung mass axle 1	m_{u1}	500 kg
Unsprung mass axle 2	m_{u2}	500 kg
Length of the vehicle	L_v	11.25 m
Axle spacing	A_s	7.6 m
Tyre 1 stiffness	$K_{t,1}$	1.75×10^6 N/m
Tyre 2 stiffness	$K_{t,2}$	3.5×10^6 N/m
Damper 1 stiffness	$K_{s,1}$	4×10^5 N/m
Damper 2 stiffness	$K_{s,2}$	10^6 N/m
Damper 1 damping	$C_{s,1}$	10^3 Ns/m
Damper 2 damping	$C_{s,2}$	2×10^3 Ns/m
Centre of gravity distance from axle 1	D_1	3.8 m
Centre of gravity distance from axle 2	D_2	3.8 m
Height of the vehicle	h	3.76 m
Constant velocity	c	72 km/h (20 m/s)

Table 2. Geometrical and mechanical properties of the modelled bridge

Bridge Property	Notation	Value
Number of elements	N	40
Frequency	f_s	1000 Hz
Length	L	20 m
Young's modulus	E	3.5×10^{10} N/m^2
2nd moment of area	I	1.26 m^4
Mass per unit length	μ	37500 kg/m
Damping	ξ	3%
First natural frequency	f_1	4.26 Hz
Length of the approach	L_{app}	10 m

OBrien et al. propose IC in [48], which is calculated using the deflections measured at three locations. The distance between the measurement points, Δx=1 m, is constant (Fig. 1).

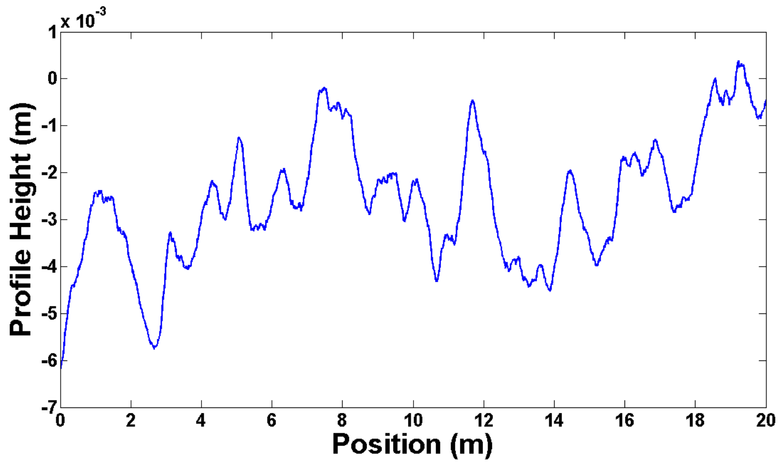

Figure 2. Bridge's road profile

Curvature is defined as the second derivation of the deflection with respect to distance and is found from a central difference approximation:

$$IC(x,t) = \frac{u(x-\Delta x,t) - u(x,t) + u(x+\Delta x,t)}{\Delta x^2} \quad (15)$$

where t is time and u is the bridge's absolute deflection. MRC can be defined using the measurements at three different positions [48]:

$$MRC(x,t) = \frac{u(x-\Delta x,t-\Delta t) - u(x,t) + u(x+\Delta x,t+\Delta t)}{\Delta x^2} \quad (16)$$

For both IC and MRC, position changes with time, according to the simple relation $c = \frac{\Delta x}{\Delta t}$, i.e., constant speed is assumed for the vehicle traversing the bridge. The traditional definition of curvature considers calculation at an instant of time and IC is calculated according to this definition. MRC differs from IC in that different instants of time are applicable for the three points in space used in the calculation. With MRC, a different damage identification parameter is expected.

Random noise is applied to the simulated measurements. The noisy signal, u_{noise}, is generated using Eq. 17:

$$u_{noise}(x,t) = u(x,t) + E_P \times N_{noise} \times u_{max} \quad (17)$$

where u_{max} is the maximum deflection of the bridge, E_P is the noise level (0 for 0% noise and 1 for 100% noise) and N_{noise} is a random vector with zero mean value and unit standard deviation. It has been assumed here that the noise in each sensor is independent. As curvature is the 2[nd] derivative of deflection, this assumption has significant implications for accuracy. Any differences in the road profile between successive measurements are deemed to be included in the noise.

Results and discussion

Damage is modelled as a loss of stiffness in selected elements of the FE model. A point damage case (A) and a multiple-point damage case (B) are studied as shown in Fig 3. 20% and 50% losses of stiffness are considered in each case.

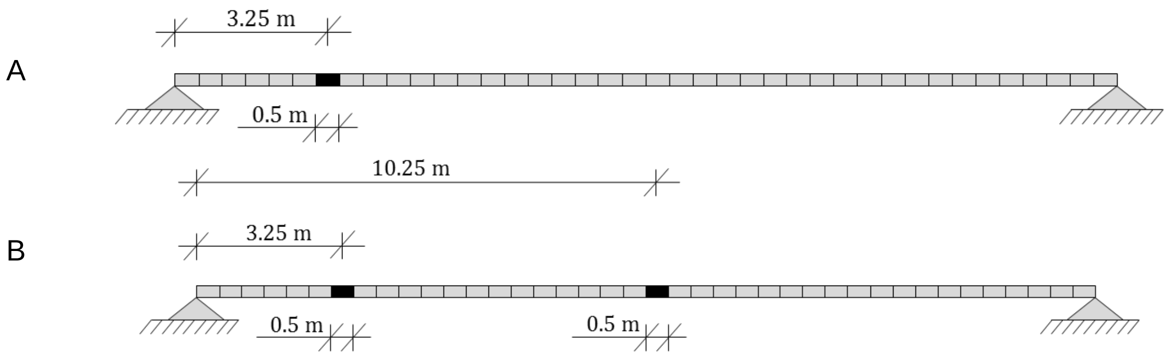

Figure 3. The damage cases.

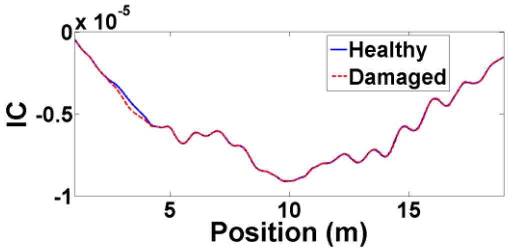

(a) No noise, 20% damage

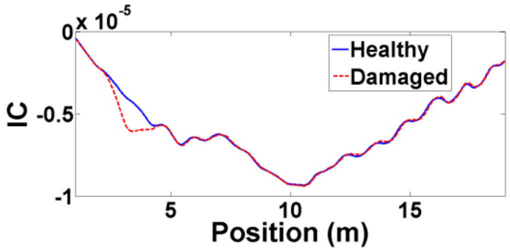

(b) No noise, 50% damage

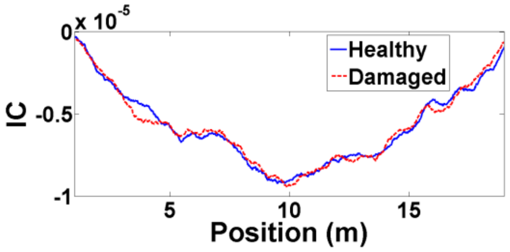

(c) 1% noise, 20% damage

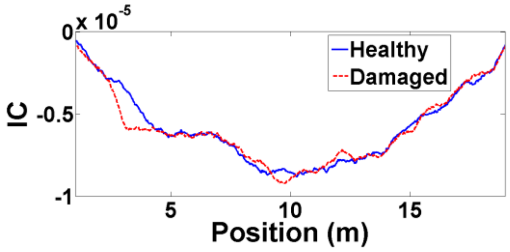

(d) 1% noise, 50% damage

Figure 4. ICs for damage case A

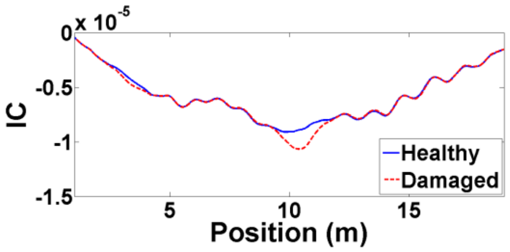

(a) No noise, 20% damage

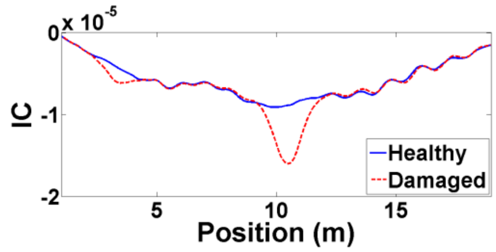

(b) No noise, 50% damage

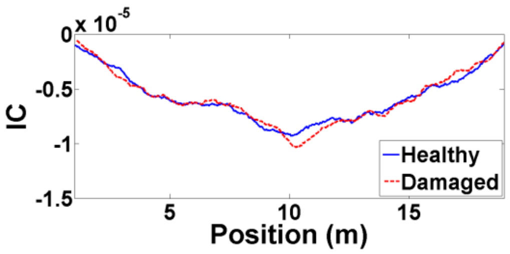

(c) 1% noise, 20% damage

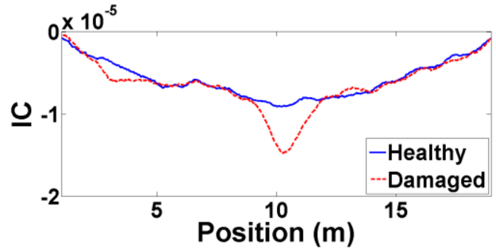

(d) 1% noise, 50% damage

Figure 5. ICs for damage case B

The vehicle is simulated to pass over the bridge and the deflection responses are measured by the three sensors. Figs. 4 and 5 show the results of IC obtained for damage cases A and B, respectively.
It can be seen that when noise is not considered in the measurement, the change in IC due to damage is quite noticeable for these substantial levels of damage. However, with just 1% noise, the damage is hardly detectable. In order to improve the results, the vehicle is simulated to pass over the bridge 10 times and the mean IC calculated. A damage indicator is proposed based on difference ratio (DR), defined as:

$$DR(\%) = \frac{\overline{IC}_{dam} - \overline{IC}_{hea}}{\min\left(\overline{IC}_{hea}\right)} \times 100 \quad (18)$$

where $\overline{IC}_{dam}$ and $\overline{IC}_{hea}$ are the filtered mean instantaneous curvatures for the damaged and healthy bridges respectively and $\min\left(\overline{IC}_{hea}\right)$ is the minimum value of $\overline{IC}_{hea}$, considering that the values are negative. The filter used for both mean curvatures is the moving average filter, defined as:

$$m[i] = \frac{1}{P} \sum_{j=-(P-1)/2}^{(P-1)/2} y[i+j] \quad (19)$$

where $y[i+j]$ is the input signal, $m[i]$ is the filtered signal and P is the number of points used in the moving average [55]. For this particular filtering of the signal, P = 51 is considered in order to average the results over one metre. DR is calculated for both damage scenarios and shown in Fig. 6.

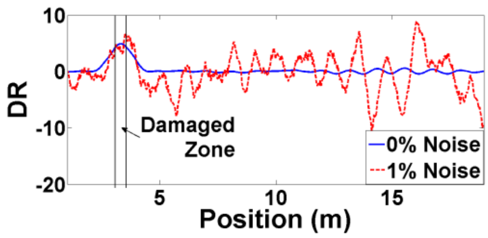

(a) Damage case A, 20% damage

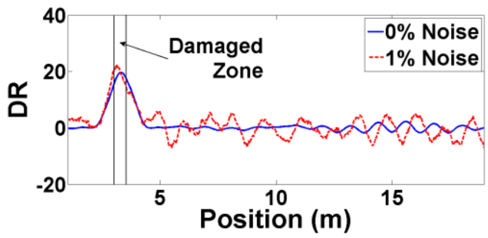

(b) Damage case A, 50% damage

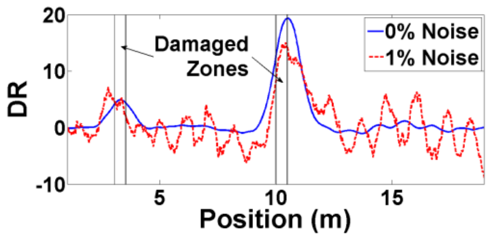

(c) Damage Case B, 20% damage

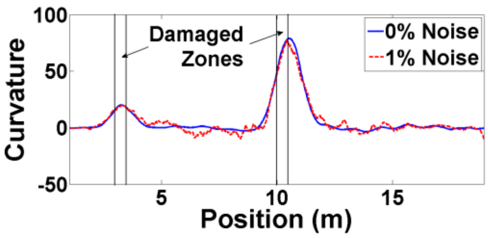

(d) Damage Case B, 50% damage

Figure 6. DR for the IC Damage Situations with 20 and 50% loss of stiffness

It can be seen that in the absence of noise, the damage location is detectable. In a noisy environment, only a large loss of stiffness is well detectable. However, the risk of having false positives is high.

Moving Reference Curvature (MRC) is also tested. One of the advantages of MRC over IC is that only 1 sensor is needed. The same sensors and the same distance, $\Delta x = 1$ m as for IC, is considered in the calculations. This distance is equivalent to a time difference of $\Delta t = 0.05\ s$, considering that velocity is $c = 20\,\frac{\text{m}}{\text{s}}$ The same moving average filtering is applied for MRC as for IC. The main drawback of MRC is the loss of local damage detection capacity as can be seen in Figs. 7 and 8. For damage case A (Fig. 7), there is no significant difference between the healthy and damaged cases at the damage location, although a small overall difference exists between the signals. For damage case B (Fig. 8), there are significant differences between the healthy and damaged cases but there is no obvious link with the damage locations.

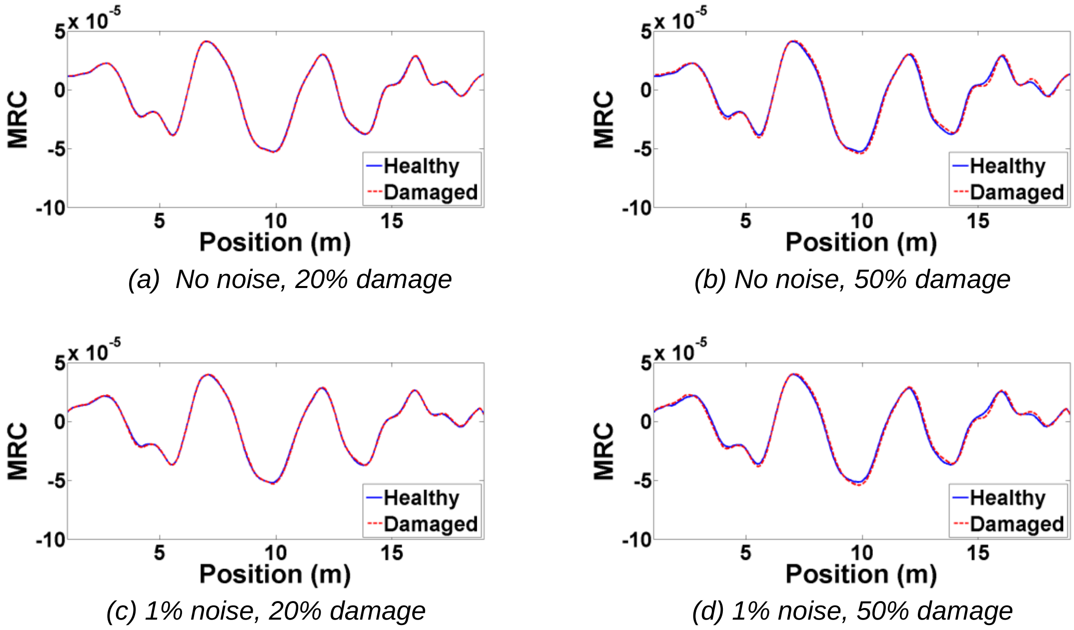

(a) No noise, 20% damage (b) No noise, 50% damage

(c) 1% noise, 20% damage (d) 1% noise, 50% damage

Figure 7. MRCs for damage case A

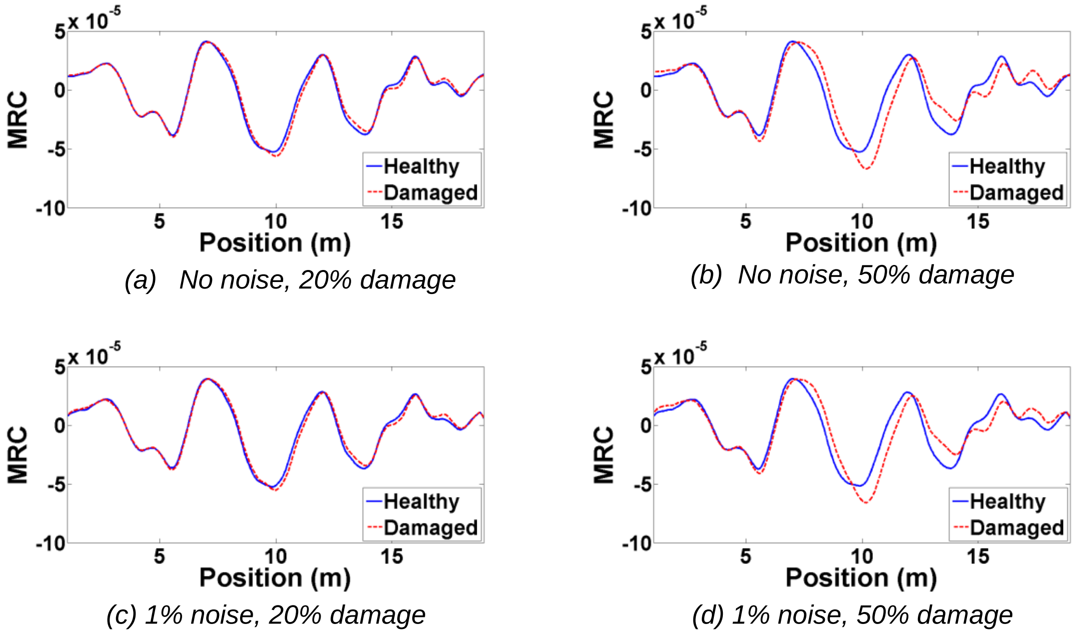

(a) No noise, 20% damage (b) No noise, 50% damage

(c) 1% noise, 20% damage (d) 1% noise, 50% damage

Figure 8 MRCs for damage case B

The root mean square (RMS) difference between the healthy and damaged signals is calculated as:

$$RMS_{MRC} = \sqrt{\sum_{i=1}^{k}(MRC_{Dam} - MRC_{Hea})^2} \quad (20)$$

where MRC_{Dam} is the MRC for the damaged case, MRC_{Hea} is the corresponding signal for the healthy case and *k* is the number of data points recorded by the TSD as it crosses the bridge. It can be seen in Table 3 that, for both damage cases, the RMS difference is non-zero and significant. It is notable that the influence of random noise is very small – clearly the influence of damage on the MRC is much greater than the influence of random noise. The cases of 50% damage give much greater RMS difference than the cases of 20% damage. Case B also gives much greater RMS difference than case A. It is concluded that RMS has potential for use as a damage detector but is not suitable for damage location.

Table 3. Root mean square of differences between healthy and damaged MRC signals.

	20% Notation		50% Notation	
	0% Noise	1% Noise	0% Noise	1% Noise
Damage A	1.4331×10^{-5}	1.8940×10^{-5}	5.7283×10^{-5}	5.7277×10^{-5}
Damage B	8.5724×10^{-5}	8.5748×10^{-5}	3.0978×10^{-4}	3.0148×10^{-4}

Although the proposed methods show promising results, there are still challenges to be addressed before they can be used in real applications. A key issue is calibrating the vehicle and dealing with any changes in vehicle properties between runs, e.g., due to suspension wear or changes in tyre pressure. Another issue is the influence of other sources of change in curvature between measurements such as frost heave or unintentional deviation in the transverse position of the vehicle causing a change in the road profile experienced by the vehicle. If such changes are random (as assumed here), they adversely affect IC but MRC still appears to work well for simple damage detection.

Conclusions

In this paper, Instantaneous Curvature (IC) is proposed for indirect detection of local damage in a bridge. A Difference Ratio (DR) between the damaged and healthy cases is proposed for damage localization. DR is shown to be effective but only when random noise is small. Random errors may occur due to measurement inaccuracy or due to changes in the road profile between measurements. MRC is easier to measure than IC, requiring only one sensor, but is less sensitive to local damage. However, it does provide the potential to detect damage and appears to have very low sensitivity to random error.

Acknowledgements

The authors acknowledge the support for the work reported in this paper from the European Union's Horizon 2020 Research and Innovation Programme under the Marie Sklodowska-Curie grant agreement No. 642453.

References

[1] C. R. Farrar, and K. Worden, "An introduction to structural health monitoring," *Philosophical Transactions of the Royal Society of London A: Mathematical, Physical and Engineering Sciences,* vol. 365, no. 1851, pp. 303-315, 2007.

[2] F.-K. Chang, *Structural health monitoring 2000*: CRC Press, 1999.

[3] H. Sohn, J. A. Czarnecki, and C. R. Farrar, "Structural health monitoring using statistical process control," *Journal of Structural Engineering,* vol. 126, no. 11, pp. 1356-1363, 2000.

[4] H. Sohn, C. R. Farrar, F. M. Hemez, D. D. Shunk, D. W. Stinemates, B. R. Nadler, and J. J. Czarnecki, "A review of structural health monitoring literature: 1996-2001," in 3rd World Conference on Structural Control, Como, Italy, 2004.

[5] A. Rytter, "Vibration Based Inspection of Civil Engineering Structures, 1993," PhD Thesis, Dept. of Building Technology and Structural Engineering, Aalborg University, Aalborg, Denmark, 1993.

[6] J. M. Brownjohn, "Structural health monitoring of civil infrastructure," *Philosophical Transactions of the Royal Society of London A: Mathematical, Physical and Engineering Sciences,* vol. 365, no. 1851, pp. 589-622, 2007.

[7] H.-N. Li, D.-S. Li, and G.-B. Song, "Recent applications of fiber optic sensors to health monitoring in civil engineering," *Engineering structures,* vol. 26, no. 11, pp. 1647-1657, 2004.

[8] E. P. Carden, and J. M. Brownjohn, "ARMA modelled time-series classification for structural health monitoring of civil infrastructure," *Mechanical systems and signal processing,* vol. 22, no. 2, pp. 295-314, 2008.

[9] J. P. Lynch, "An overview of wireless structural health monitoring for civil structures," *Philosophical Transactions of the Royal Society of London A: Mathematical, Physical and Engineering Sciences,* vol. 365, no. 1851, pp. 345-372, 2007.

[10] J. Ko, and Y. Ni, "Technology developments in structural health monitoring of large-scale bridges," *Engineering structures,* vol. 27, no. 12, pp. 1715-1725, 2005.

[11] S. Jang, H. Jo, S. Cho, K. Mechitov, J. A. Rice, S.-H. Sim, H.-J. Jung, C.-B. Yun, B. F. Spencer Jr, and G. Agha, "Structural health monitoring of a cable-stayed bridge using smart sensor technology: deployment and evaluation," *Smart Structures and Systems,* vol. 6, no. 5-6, pp. 439-459, 2010.

[12] Z. Zhou, T. W. Graver, L. Hsu, and J.-p. Ou, "Techniques of advanced FBG sensors: Fabrication, demodulation, encapsulation, and their application in the structural health monitoring of bridges," *Pacific Science Review,* vol. 5, no. 1, pp. 116-121, 2003.

[13] Z. Li, T. H. Chan, and J. M. Ko, "Fatigue analysis and life prediction of bridges with structural health monitoring data—Part I: methodology and strategy," *International Journal of Fatigue,* vol. 23, no. 1, pp. 45-53, 2001.

[14] C. Machelski, and M. Hildebrand, "Efficiency of monitoring system of a cable-stayed bridge for investigation of live loads and pier settlements," *Journal of Civil Structural Health Monitoring,* vol. 5, no. 1, pp. 1-9, 2015.

[15] F. Magalhães, Á. Cunha, and E. Caetano, "Dynamic monitoring of a long span arch bridge," *Engineering Structures,* vol. 30, no. 11, pp. 3034-3044, 2008.

[16] I. N. Robertson, "Prediction of vertical deflections for a long-span prestressed concrete bridge structure," *Engineering Structures,* vol. 27, no. 12, pp. 1820-1827, 2005.

[17] W. Fan, and P. Qiao, "Vibration-based damage identification methods: a review and comparative study," *Structural Health Monitoring,* vol. 10, no. 1, pp. 83-111, 2011.

[18] E. J. OBrien, and A. Malekjafarian, "A mode shape-based damage detection approach using laser measurement from a vehicle crossing a simply supported bridge," *Structural Control and Health Monitoring*, 2016.

[19] A. Malekjafarian, P. J. McGetrick, and E. J. OBrien, "A Review of Indirect Bridge Monitoring Using Passing Vehicles," *Shock and Vibration,* vol. 2015, pp. 16, 2015.

[20] Y.-B. Yang, C. Lin, and J. Yau, "Extracting bridge frequencies from the dynamic response of a passing vehicle," *Journal of Sound and Vibration,* vol. 272, no. 3, pp. 471-493, 2004.

[21] Y. Yang, and C. Lin, "Vehicle–bridge interaction dynamics and potential applications," *Journal of sound and vibration,* vol. 284, no. 1, pp. 205-226, 2005.

[22] E. J. OBrien, A. Malekjafarian, and A. González, "Application of empirical mode decomposition to drive-by bridge damage detection," *European Journal of Mechanics-A/Solids,* vol. 61, pp. 151-163, 2017.

[23] C. Bowe, P. Quirke, D. Cantero, and E. J. O'Brien, "Drive-by structural health monitoring of railway bridges using train mounted accelerometers." pp. 1652-1663.

[24] D. Martinez, E. J. OBrien, and E. Sevillano, "Damage Detection by Drive-by Monitoring Using the Vertical Displacements of a Bridge," in Sixth International Conference on Structural Engineering, Mechanics and Computation (SEMC 2016), Cape Town, South Africa, 5 to 7 September 2016, 2016, pp. 1915-1918.

[25] E. J. OBrien, and J. Keenahan, "Drive-by damage detection in bridges using the apparent profile," *Structural Control and Health Monitoring,* vol. 22, no. 5, pp. 813-825, 2015.

[26] C.-W. Kim, R. Isemoto, T. Toshinami, M. Kawatani, P. McGetrick, and E. J. O'Brien, "Experimental investigation of drive-by bridge inspection," in 5th International Conference on Structural Health Monitoring of Intelligent Infrastructure (SHMII-5), 11-15 December, 2011, Cancun, Mexico, 2011.

[27] A. Malekjafarian, and E. J. OBrien, "Application of output-only modal method in monitoring of bridges using an instrumented vehicle," in S. Nanukuttan and J. Goggins, eds., Civil Engineering Research in Ireland, Belfast, UK, 28-29 August, 2014.

[28] O. S. Salawu, "Detection of structural damage through changes in frequency: A review," *Engineering Structures,* vol. 19, no. 9, pp. 718-723, Sep, 1997.

[29] J.-T. Kim, and N. Stubbs, "Crack detection in beam-type structures using frequency data," *Journal of Sound and Vibration,* vol. 259, no. 1, pp. 145-160, 2003.

[30] J.-T. Kim, Y.-S. Ryu, H.-M. Cho, and N. Stubbs, "Damage identification in beam-type structures: frequency-based method vs mode-shape-based method," *Engineering structures,* vol. 25, no. 1, pp. 57-67, 2003.

[31] R. Curadelli, J. Riera, D. Ambrosini, and M. Amani, "Damage detection by means of structural damping identification," *Engineering Structures,* vol. 30, no. 12, pp. 3497-3504, 2008.

[32] A. González, E. J. OBrien, and P. J. McGetrick, "Identification of damping in a bridge using a moving instrumented vehicle," *Journal of Sound and Vibration,* vol. 331, no. 18, pp. 4115-4131, 2012.

[33] J. N. Yang, Y. Lei, S. Lin, and N. Huang, "Hilbert-Huang based approach for structural damage detection," *Journal of engineering mechanics,* vol. 130, no. 1, pp. 85-95, 2004.

[34] A. Malekjafarian, and E. J. OBrien, "Identification of bridge mode shapes using Short Time Frequency Domain Decomposition of the responses measured in a passing vehicle," *Engineering Structures,* vol. 81, pp. 386-397, 2014.

[35] M. A. Wahab, and G. De Roeck, "Damage detection in bridges using modal curvatures: application to a real damage scenario," *Journal of Sound and Vibration,* vol. 226, no. 2, pp. 217-235, 1999.

[36] D. Hester, and A. González, “A wavelet-based damage detection algorithm based on bridge acceleration response to a vehicle,” *Mechanical Systems and Signal Processing,* vol. 28, pp. 145-166, 2012.

[37] J.-H. Park, J.-T. Kim, D.-S. Hong, D. Mascarenas, and J. P. Lynch, “Autonomous smart sensor nodes for global and local damage detection of prestressed concrete bridges based on accelerations and impedance measurements,” *Smart Structures and Systems,* vol. 6, no. 5_6, pp. 711-730, 2010.

[38] M.-Y. Choi, and I.-B. Kwon, “Damage detection system of a real steel truss bridge by neural networks,” in SPIE's 7th Annual International Symposium on Smart Structures and Materials, Newport Beach, CA, 2000, pp. 295-306.

[39] F. N. Catbas, M. Gul, and J. L. Burkett, “Conceptual damage-sensitive features for structural health monitoring: laboratory and field demonstrations,” *Mechanical Systems and Signal Processing,* vol. 22, no. 7, pp. 1650-1669, 2008.

[40] Y. Zhang, S. T. Lie, and Z. Xiang, “Damage detection method based on operating deflection shape curvature extracted from dynamic response of a passing vehicle,” *Mechanical Systems and Signal Processing,* vol. 35, no. 1, pp. 238-254, 2013.

[41] Z. Sun, T. Nagayama, D. Su, and Y. Fujino, “A Damage Detection Algorithm Utilizing Dynamic Displacement of Bridge under Moving Vehicle,” *Shock and Vibration,* vol. 2016, pp. 9, 2016.

[42] Z. A. Jassim, N. N. Ali, F. Mustapha, and N. A. Jalil, “A review on the vibration analysis for a damage occurrence of a cantilever beam,” *Engineering Failure Analysis,* vol. 31, pp. 442-461, 2013.

[43] J.-H. Kim, F. Pierron, M. Wisnom, and K. Syed-Muhamad, “Identification of the local stiffness reduction of a damaged composite plate using the virtual fields method,” *Composites Part A: Applied Science and Manufacturing,* vol. 38, no. 9, pp. 2065-2075, 2007.

[44] S. Rasmussen, L. Aagaard, S. Baltzer, and J. Krarup, “A comparison of two years of network level measurements with the Traffic Speed Deflectometer,” in Transport Research Arena Europe, Ljubljana, Slovenia, 2008, pp. 8.

[45] S. Rasmussen, J. A. Krarup, and G. Hildebrand, “Non-contact deflection measurement at high speed,” in The 6nd International Conference on the Bearing Capacity of Roads, Railways and Airfields, Lisbon, Portugal, 2002, pp. 8.

[46] G. R. Rada, S. Nazarian, B. A. Visintine, R. V. Siddharthan, and N. Sivaneswaran, “Use of High-Speed Deflection Devices in Network-Level PMS Applications: Are We Ready?,” in 9th International Conference on Managing Pavement Assets, Alexandria, Virginia, EEUU, 2015.

[47] M. Nasimifar, S. Thyagarajan, R. V. Siddharthan, and N. Sivaneswaran, “Robust Deflection Indices from Traffic-Speed Deflectometer Measurements to Predict Critical Pavement Responses for Network-Level Pavement Management System Application,” *Journal of Transportation Engineering,* vol. 142, no. 3, pp. 11, 2016.

[48] E. J. OBrien, E. Sevillano, and D. Martinez, “Monitoring the Condition of a Bridge using a Traffic Speed Deflectometer Vehicle Travelling at Highway Speed,” in 3rd International Balkans Conference on Challenges of Civil Engineering3rd International Balkans Conference on Challenges of Civil Engineering, Tirana, Albania, 2016, pp. 107-115.

[49] A. Malekjafarian, and E. J. OBrien, “On the use of a passing vehicle for the estimation of bridge mode shapes,” *Journal of Sound and Vibration,* vol. 397, pp. 77-91, 2017.

[50] D. Cebon, *Handbook of vehicle-road interaction*, 1999.

[51] D. Martinez, E. OBrien, and E. Sevillano, “Damage Detection by Drive-by Monitoring Using the Vertical Displacements of the Bridge,” in SEMC 2016, Cape Town, South Africa, 2016, pp. 5.

[52] Y. W. Kwon, and H. Bang, *The finite element method using MATLAB*: CRC press, 2000.

[53] R. W. Clough, and J. Penzien, *Dynamics of Structures*: New York, McGraw-Hill, Inc, 1993.

[54] J. W. Tedesco, W. G. McDougal, and C. A. Ross, *Structural dynamics: theory and applications*: Addison-Wesley Montlo Park, California, 1999.
[55] S. W. Smith, *The scientist and engineer's guide to digital signal processing*, 1997.